Journal of Rehabilitation in Civil Engineering 9-1 (2021) 102-113

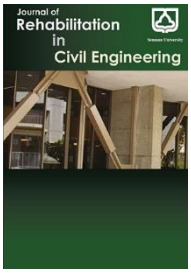

journal homepage: http://civiljournal.semnan.ac.ir/

The Punching Shear Capacity Estimation of FRP-Strengthened RC Slabs Using Artificial Neural Network and Group Method of Data Handling

E. Darvishan[1*]

1. Assistant Professor, Department of Civil Engineering, Roudehen Branch, Islamic Azad University, Roudehen, Iran

Corresponding author: *darvishan@riau.ac.ir*

ARTICLE INFO

Article history:
Received: 04 May 2020
Accepted: 05 October 2020

Keywords:
Punching shear,
RC Slab,
FRP,
Artificial Neural Network,
Group Method of Data Handling

ABSTRACT

Recently soft computing methods have been employed in most fields, especially in civil engineering, due to its high accuracy to predict the results and process information. Soft computing is the result of new scientific endeavors that make modeling, analysis, and, ultimately, the control of complex systems possible with greater ease and success. The essential methods of soft computing are fuzzy logic, artificial neural networks, and genetic algorithm. In this paper, using 74 valid experimental data, estimation of punching shear capacity of FRP-strengthened RC slabs using two powerful methods (artificial neural network and Group method of data handling) has been investigated. The maximum and minimum dimension of column cross-section, the effective height of slab, the compressive strength of concrete, modulus of elasticity of FRP bar, and the percentage of FRP bars were selected as input variables, and the punching shear capacity of the slab was selected as the output variable. Also, in order to investigate the effect of the variables mentioned above on the results, sensitivity analysis is conducted in both methods. Absolute Fraction of Variance for the two methods showed that the GMDH method had higher precision (1.73%) than the ANN method in the prediction of results.

1. Introduction

Concrete slabs are used to construct various structures with different applications, as well as decks of different bridges and flooring. Suspended slabs transfer loads by their flexural performance and separate the upper and lower spaces. These slabs include one-way, two-way, waffle, and flat ones along with flat-slab floors. A wealth of experimental and numerical studies are conducted so far on reinforced concrete slabs and strengthening of them using FRPs, with some requirements and equations provided.

Metwally [1] used an artificial neural network to estimate the shear capacity of concrete slabs reinforced with FRP bars. He concluded that the artificial neural network had better performance in predicting shear capacity compared to formula-based methods, and it could be used as a practical

DOI: 10.22075/JRCE.2020.20335.1407

tool to estimate the shear capacity. Hassan et al. [2] tested ten slab-column specimens made with longitudinal and transverse FRP bars on a real scale and evaluated their punching shear behavior. Durucan and Anil [3] investigated the punching shear of two-way slabs with opening, reinforced with CRFP. They tested various opening sizes and locations. Azimi determined the punching shear capacity of FRP-reinforced concrete slabs using GMDH and indicated that it was a very useful modeling method for the prediction of the punching shear capacity of slabs [4]. Specifically, group method of data handling (GMDH) can be considered as a powerful modeling method for civil and structural engineering pheromones [5–8]. Akbarpour et al. [9] employed an artificial neural network and ANFIS system to estimate the shear capacity of two-way slabs. For this purpose, they collected 189 specimens, developed the two models, and found that both models were able to predict the shear capacity of two-way slabs with high accuracy. Hassan et al. [10] conducted an experimental study to enhance the punching shear strength of reinforced concrete slabs by strengthening them by shear metal strips. They made seven full-scale specimens and subjected them to gravitational loading. Akhundzada et al. [11] examined different methods of strengthening slab-column connections with CFRP sheets to avoid punching shear. They concluded that strengthening improved the ultimate load by 25% and reduced the maximum deflection by up to 50%. Marí et al. [12] introduced a mechanical model for reinforced concrete slabs based on previous experimental results. Hamdy et al. [13] studied the effectiveness of using shear bolts to reduce the punching shear of concrete slabs. Gokkus et al. implemented Artificial Neural Network (ANN) for predicting the required concrete volume and amount of the steel reinforcement within the inversed-T-shaped and stem-stepped reinforced concrete (RC) walls [14]. They have shown that pattern recognition using ANN can provide precise and robust models [14]. Wu et al. [15] conducted a numerical study on the strengthening of flat RC slabs with FRP laminates and proposed a model to which could meet the analysis results. Using artificial intelligence, including artificial neural network (ANN) and gene expression programming (GEP), Naderpour et al. [16] could present a model to predict the compressive strength of columns strengthened with FRP. Azizi and Talaeitaba [17] assessed a new numerical method for CFRP reinforced concrete slabs. This method included grooving in two orthogonal directions under the slab, mounting external bars, and attaching FRPs to the surface of the groove in another direction. The obtained results demonstrated the high efficiency of this method. The failure mode of strengthened specimens also changed from shear to flexure–shear.

Generally, soft computing and machine learning approaches has been successfully employed by other researchers in order to model and present the governing patterns in civil engineering problems [7,18–22].

In this study, the empirical relationships are provided to predict punching shear of reinforced concrete (RC) slabs at first. Then, using valid experimental data on RC slabs strengthened with FRP, their punching shear is predicted using an artificial neural network (ANN) and the group method of data handling (GMDH). Ultimately, using sensitivity analyses of both models, the effect of each variable on the results is determined.

2. Existing Empirical Relationships

The ACI318-11 code [23] suggests Eq. (1) to estimate the punching shear capacity of reinforced concrete slabs:

$$V_C = 0.33\sqrt{f'_c}\, b_0 d \qquad (1)$$

In which, V_c is punching shear capacity, b_0 is the perimeter of the critical section at a distance of $d/2$ from the load location, and d is the effective depth of the concrete slab.

The recommended equation of the BS8110-97 code [24] is as follows:

$$V_C = 0.79(100\rho_s)^{1/3}\left(\frac{400}{d}\right)^{1/4}\left(\frac{f_{ck}}{25}\right)^{1/3} b_0 d \qquad (2)$$

Where f_{ck} is the compressive strength of cubic specimen, ρ_s is the ratio of steel rebars, and b_0 is the perimeter of the critical section.

ACI440.1R-06 [25] suggests the Eq. (3) to estimate punching shear capacity of FRP-strengthened two-way concrete slabs, in which the effect of stiffness of the bars is accounted for in computing the shear transfer in such slabs.

$$V_C = 0.8\sqrt{f'_c}\, b_0 c$$

$$c = kd$$

$$k = \sqrt{2\rho_f n_f + (\rho_f n_f)^2} - \rho_f n_f$$

$$n_f = \frac{E_f}{E_c} \qquad (3)$$

$$\rho_f = \frac{A_f}{bd}$$

$$E_C = 4700\sqrt{f'_C}\,(MPa)$$

In this equation, b_0 and C are the critical perimeters at a distance of $d/2$ from the load and neutral axis depth in the cracked section, respectively.

Adding $\left(\frac{E_f}{E_s}\right)^{1/3}$ to the equation of the ACI318 code, El-Ghandour et al. [26] achieved the following equation:

$$V_C = 0.33\sqrt{f'_c}\left(\frac{E_f}{E_s}\right)^{1/3} b_0 d \qquad (4)$$

In which E_f and E_s are the elastic moduli of the FRP and steel, and the other parameters are defined as those of Eq. 1.

The equation introduced by Matthys and Taerwe [27], which is the modified form of the BS8110 equation, is

$$V_C = 1.36\frac{(100\rho_f \frac{E_f}{E_s} f'_c)^{1/3}}{d^{1/4}} b_0 d \qquad (5)$$

In this equation, ρ_f, E_f, and E_s are the ratio of FRP bars and elastic moduli of the FRP and steel, respectively. The other variables are the same as those of Eq. 2.

Ospina et al. [28] modified the relationship of Matthys and Taerwe as the following.

$$V_C = 2.77(\rho_f f'_c)^{1/3}\sqrt{\frac{E_f}{E_s}}\, b_0 d \qquad (6)$$

El-Gamal et al. [29] improved the ACI318 equation by taking into account the effect of flexural stiffness $(\rho_f \times E_f)$ of the bottom primary reinforcement and suggested the following equation.

$$V_C = 0.33\sqrt{f'_c}\, b_0 d\alpha(1.2)^N \qquad (7)$$

In this equation, N denotes the effect of slab continuity. α show the effect of flexural

stiffness of the reinforcement, loading area, and effective depth of the slab

$$\alpha = 0.62 \times (\rho_f E_f)^{1/3} \times (1 + \frac{8d}{b_0}) \quad (8)$$

Where ρ_f and E_f are the steel ratio and elastic modulus of the rebars, respectively, other parameters are the same as those of Eq. 1.

Kurtoglu et al., considering the slab directions, achieved the equation below using the gene expression programming algorithm.

$$P = \frac{0.0862 c^{0.391} d^{1.6} f_c^{0.2} E_F^{0.2} \rho^{0.354}}{L^{0.2}} \quad (9)$$

In which, C and d denote the square column dimension, and effective depth of the concrete slab, respectively. Also, f_c, E_f, ρ, and L are the compressive strength of concrete, the elastic modulus of FRP, reinforcement percentage, and concrete slab depth, respectively.

3. Methods

3.1. Artificial Neural Networks

An artificial neural network (ANN) is a system inspired by humans' brains. The biological network is made of neurons that interact with each other to process information. Each neuron makes decisions by receiving the input and producing output. Dendrite gets input signal and transfers it to the cell body. If the input signals reach a predefined value, the cell body fires and transfers the input to the neighbor dendrites through the axon. Neurons are connected in series and parallel. Therefore they can make complex decisions. Accordingly, the artificial neuron works with three basic terms: weight, bias and activation function. All the inputs are multiplied by their corresponding weights and then sum up. Weights adjust the strength of the signal, and biases add an additional input to the neuron.

Table 1. References of data used for analysis Presentation of the model.

No.	Reference	Number of used data
1	Banthia et al. [30]	2
2	Matthys and Taerwe [27]	13
3	El-Ghandour et al. [26]	5
4	Ospina et al. [28]	3
5	Lee et al. [31]	3
6	Ahmed et al. [32]	4
7	El-Gamal et al. [33]	5
8	Rahman et al. [34]	1
9	Hassan et al. [35]	1
10	Hussein and Rashid [36]	4
11	Zaghloul and Razaqpur [37]	1
12	Bouguerra et al. [38]	6
13	Ramzy et al. [39]	4
14	Dulude et al. [40]	11
15	Hassan et al. [41]	8
16	Nguyen-Minh and Rovňák [42]	3

Table 2. Effective parameters in the behavior of FRP reinforced slabs.

parameter	description
$C_x\,(mm)$	size of the large side of the column
$C_y\,(mm)$	size of the small side of the column
$d\,(mm)$	the effective depth of the slab
$f_c^{'}\,(MPa)$	strength of the cylindrical specimen
$E_f\,(GPa)$	Elastic modulus of FRP rebar
$\rho_f\,(\%)$	FRP rebar percentage
$V_{test}\,(kN)$	test punching shear capacity

Activation function is used to the neuron to be able to perform map nonlinear mappings. Since a simple neuron is not able to make complex decisions, a network consists of parallel layers of neurons. On this basis, a network usually have input, hidden, and output layers. To train a network (i.e., selecting the proper weights and biases),

backpropagation is the most popular algorithm. It can learn faster and is more effective than other algorithms [43].

3.2. Modeling with GDMH Method

The GMDH includes a bin of neurons formed by a quadratic polynomial. By combining the polynomials, the network describes the approximate function $\hat{f}$ with the output $\hat{y}$ for a given input, $x=\{x_1,x_2,x_3,....\}$, in comparison to the real output y. M observations which contain n inputs and the output of real values are as the following:

$$y_i = f\left(x_{i1},x_{i2},x_{i3},\ldots,x_{in}\right)\left(i=1,2,\ldots,M\right) \quad (10)$$

We are searching for a network by which the error between the real output and the predicted one is minimized

$$\sum_{i=1}^{M}(\hat{y}_i - y_i)^2 \rightarrow \min \quad (11)$$

The polynomial function between input and output is usually stated by Volterra function as

$$y = a_0 + \sum_{n}^{1} a_i x_i + \sum_{n}^{1}\sum_{n}^{1} a_{ij} x_i x_j + \sum_{n}^{1}\sum_{n}^{1}\sum_{n}^{1} a_{ijk} x_i x_j x_k + \ldots \quad (12)$$

Which is also called the Kolmogorov-Gabor polynomial. In most practical cases, a second-class form with two variables of this function is employed

$$\hat{y} = G\left(x_i,x_j\right) = a_0 + a_1 x_i + a_2 x_j + a_3 x_i x_j + a_4 x_i^2 + a_5 x_j^2 \quad (13)$$

The coefficients of a_i are determined by least-square methods. The coefficients of G_i can be calculated by fitting the output in the input-output pair so that the error of squares is minimized.

Table 3. Statistical properties of input and output data.

	$C_x\,(mm)$	$C_y\,(mm)$	$d\,(mm)$	$f_c^{'}\,(MPa)$	$E_f\,(GPa)$	$\rho_f\,(\%)$	$V_{test}\,(kN)$
max	450	600	284	118	3.78	147.6	1600
min	75	75	55	26	0.18	28.4	61
mean	236.22	294.32	132.83	40.77	0.99	64.93	436.90
Standard dev.	89.26	161.02	50.39	13.10	0.71	31.66	349.05
range	375	525	229	92	3.6	119.2	1539

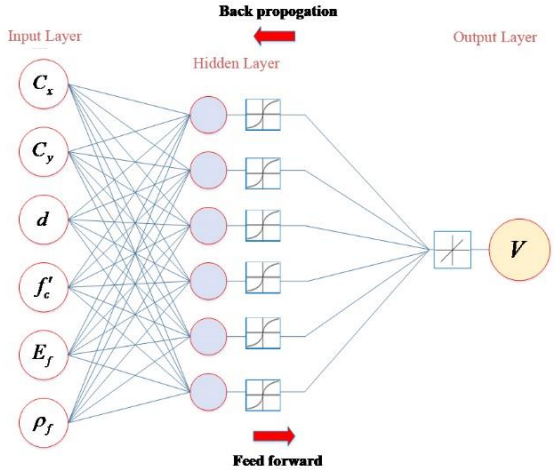

Fig. 1. Schematic view of the artificial neural network.

$$E = \frac{\sum_{i=1}^{M}(y_i - G_i)^2}{M} \rightarrow \min \quad (14)$$

Usually, GMDH algorithms use double combinations of n input variables and using regression, and polynomial regression equations are obtained

$$\binom{n}{2} = \frac{n(n-1)}{2} \quad (15)$$

By the given input and output variables, the Eq. 12 can be written in the matrix form

$$A\mathbf{a} = Y \tag{16}$$

where A is the vector of unknown weight coefficients and Y is the vector of output variables

$$\mathbf{a} = \{a_0, a_1, a_2, a_3, a_4, a_5\}$$
$$Y = \{y_1, y_2, y_3, \ldots, y_M\}^T \tag{17}$$
$$A = \begin{bmatrix} 1 & x_{1p} & x_{1q} & x_{1p}x_{1q} & x_{1p}^2 & x_{1q}^2 \\ 1 & x_{2p} & x_{2q} & x_{2p}x_{2q} & x_{2p}^2 & x_{2q}^2 \\ \cdots & \cdots & \cdots & \cdots & \cdots & \cdots \\ 1 & x_{Mp} & x_{Mq} & x_{Mp}x_{Mq} & x_{Mp}^2 & x_{Mq}^2 \end{bmatrix}$$

Regression equations obtain a vector of weights coefficients in matrix form

$$\mathbf{a} = (A^T A)^{-1} A^T Y \tag{18}$$

These steps are repeated for every neuron in the hidden layers [44]

4. Modeling

In this paper, a model is proposed using 74 valid experimental specimens with an artificial neural network and the group method of data handling. Table 2 introduces the input parameters of the network. The network inputs and goals were normalized to achieve efficient results in training the neural network. For instance, Eq. 19 was used to scale the effective depth of the concrete slab (d):

$$d_{scaled} = \left[(0.9-0.1)\times\frac{(d-d_{\min})}{(d_{\max}-d_{\min})}\right]+0.1 \tag{19}$$

Where d_{min} and d_{max} are the minimum and maximum effective depths of concrete slab, obtained from Table 3. Table 2 lists the references used for the modeling, as well as the number of specimens chosen from each of them.

Fig. 2. Regression values in different hidden layers.

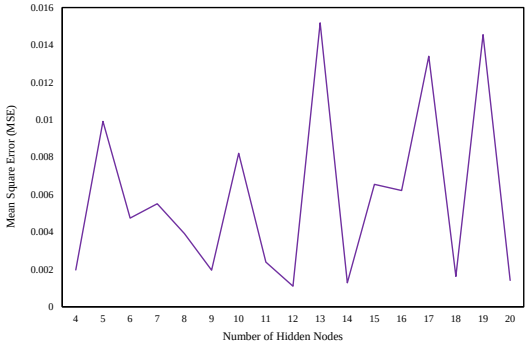

Fig. 3 Mean of squared error in different hidden layers

4.1. Artificial Neural Network (ANN)

The backpropagation network consists of one input layer. The number of network inputs indicates the number of parameters existing in the input section. It also has one or more hidden layers with several neurons. The logarithmic sigmoid equation was employed in the hidden layer, while a simple linear function was employed in the output layer. TRAINLM and LEARNGDM were used as the training function and adaption learning function, respectively. Networks with 4 to 20 hidden neurons were formed to find a proper one. Fig. 1 shows a schematic of different layers, including input, hidden, and output ones in the neural network.

The values of mean square error (MSE) and regression for different hidden neurons are shown in Figs. 2 and 3, respectively. As the

MSE and regression values of a network are lower and closer to one, respectively, it acts better in predicting the results. Therefore, by examining the MSE and regression values for different numbers of hidden neurons shown in Figs. 2 and 3, the network with 12 hidden neurons was found to have the least MSE values while its regression values were close to one, so it was chosen as the optimum one.

Fig. 4 illustrates the MSE values in various learning epochs. According to the considered convergence criterion, it can be seen that learning in epoch 7 was well done. The trend of network changes during different epochs is shown in Fig. 5. Fig. 6 demonstrates the values of R obtained for four modes of training, verification, testing, and entire data. The higher concentration of these points on the bisector of the first quarter indicates its higher accuracy.

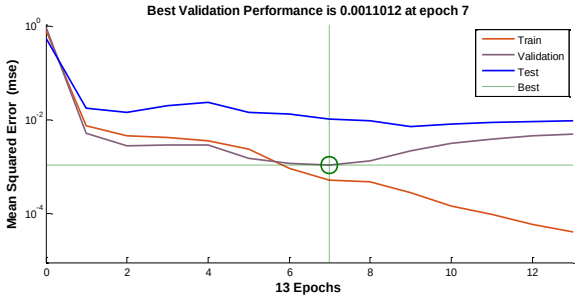

Fig. 4. MSE for the training process.

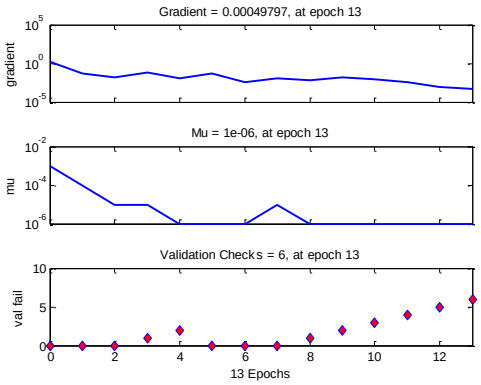

Fig. 5. Error estimation in the validation process.

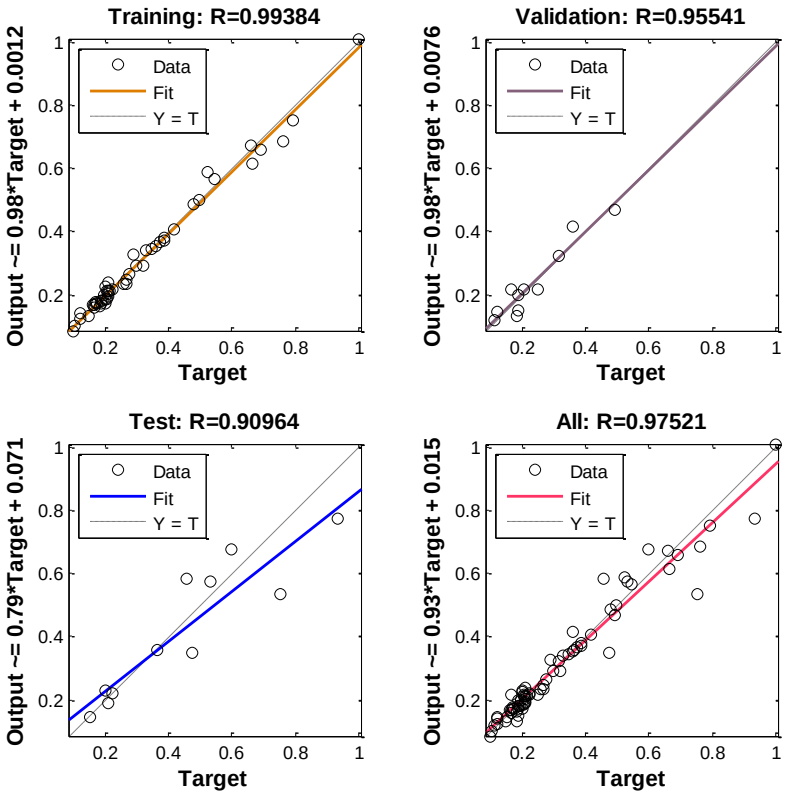

Fig. 6. Regression curve of the network after training.

4.2. Group Method of Data Handling

The GMDH was used for modeling in addition to the artificial neural network in this study. By using this method, the nonlinear links and relationships between the data can be found, and a model with high prediction capacity can be created. Moreover, GMDH Shell does not need the normalization scale of data and considerably reduces the calculation time. The goal of modeling with GMDH neural networks was to find a $\hat{f}$ function, which can calculate the output for the input $x=\{x_1, x_2, x_{3,\ldots\ldots}\}$. The values predicted by GMDH, along with those obtained from the tests, are plotted in Fig. 7 to give a better understanding of the performance of the chosen optimum network. The error rate for each prediction is also shown in Fig. 8. As can be seen, the values predicted by this method were very close to the real ones.

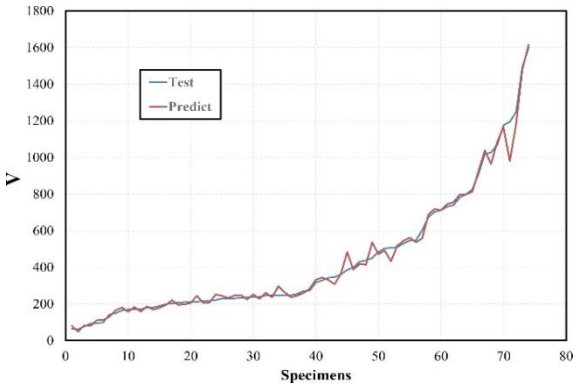

Fig. 7. Comparison of estimated values of GMDH and test results.

In order to evaluate the performance of the two presented models and their accuracy in predicting the experimental results, different performance criteria, such as mean absolute percentage error (MAPE) and the absolute fraction of variance (R^2), were used whose values for both models are presented in Table 4. According to this table, the maximum and minimum error rates in the GMDH model were respectively lower and higher than those in the ANN model. As R^2 is closer to one and MAPE has a lower value, the model has higher accuracy in predicting the results. Hence, the GMDH model was more accurate than the ANN model.

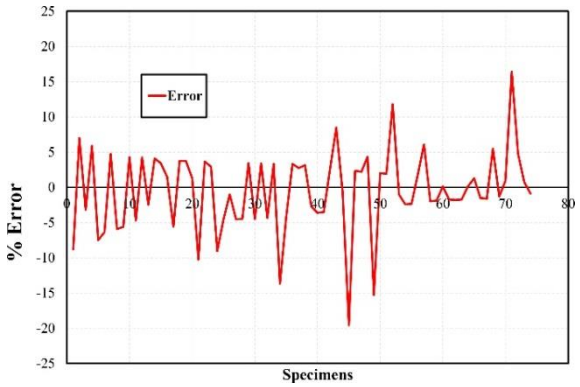

Fig. 8. Error percentage in the estimation of results.

Table 4. Statistical properties of input and output data.

model	min error	max error	error std	Coeff. of var.	R^2	MAPE
ANN	0.035	33	7.57	0.94	0.98	8.05
GMDH	0. 126	19.57	3.73	0.86	0.997	4.32

$$R^2 = 1 - \frac{\sum_{i=1}^{N}\left(V_{(actual)} - V_{(\text{model})}\right)^2}{\sum_{i=1}^{N}\left(V_{(pedict)}\right)^2}$$

$$MAPE = \frac{1}{M}\left[\frac{\sum_{i=1}^{M}\left|V_{(\text{mod}el)} - V_{(actual)}\right|}{\sum_{i=1}^{M} V_{(actual)}} \times 100\right] \quad (20)$$

5. Sensitivity Analysis of the Input Parameters

The sensitivity analysis expresses how and to what extent each input affects the provided equation. The analysis is based on weights to estimate the impact of each input data on the output data in the network. Various equations have been suggested according to the values of weights. The Milne equation [45] is one of the most practical ones. By calculating the weights w_{ji} (weight of the link between input neuron i and hidden neuron j) multiplied by w_{oj} (weight of the link) for each hidden neuron of the network, this equation is obtained as the sum of the calculated products.

$$Q_{ik} = \frac{\sum_{j=1}^{nhidden} \frac{w_{ji}}{\sum_{l=1}^{ninputs} |w_{jl}|} . w_{oj}}{\sum_{k=1}^{ninputs} \left(\sum_{j=1}^{nhidden} \left| \frac{w_{jk}}{\sum_{l=1}^{ninputs} |w_{jl}|} . w_{oj} \right| \right)} \quad (21)$$

In Eq. 21, $\sum_{l=1}^{ninputs} |w_{jl}|$ is the sum of the link's weights, and Q_{ik} is the percent of the effect of the input variable x_i on the output variable y_k. Correct ratios for both positive and negative weights are obtained using this method.

$iw\{1,1\}$ and $iw\{2,1\}$ are the weight of the input and output parameters, respectively. As can be seen in Fig. 9, the effects of parameters on the output were almost equal. However, the small dimension of the column, the large dimension of the column, and the effective depth of the concrete slab had the highest effects on the lateral confinement coefficient, being 18.64%, 17.82%, and 16.95%, respectively. Meanwhile, the elastic modulus of the FRP bar had the lowest effect on the output parameter, being 14.97%.

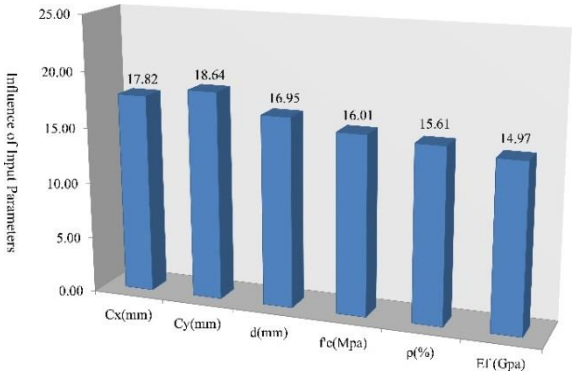

Fig. 9 The effect of input variables on output values in the model

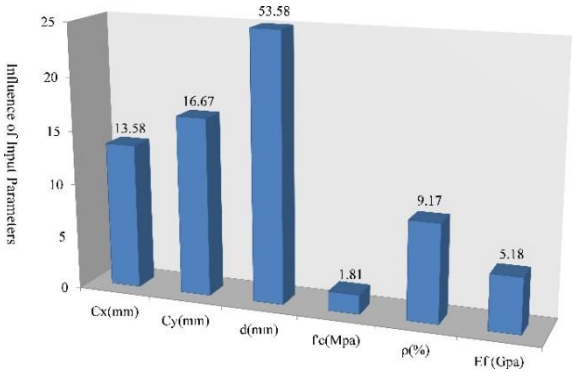

Fig. 10. The effect of input variables on output values in GMDH model.

The sensitivity analysis of the model constructed by GMDH is shown in Fig. 10. As can be seen, the parameters of the effective depth of the concrete slab, the small dimension of the column, and the large dimension of the column had the highest effects on the output parameter, respectively. On the other hand, the parameters of the FRP reinforcement ratio, the elastic modulus of FRP bars, and the cylindrical strength of the specimens had the lowest effects.

6. Conclusions

In this study, the punching shear capacity of FRP-strengthened concrete slabs was predicted using the artificial neural network and group method of data handling. Six parameters, including the large dimension of the column, the small dimension of the column, the effective depth of the slab, the

strength of the cylindrical concrete specimen, the elastic modulus of the FRP bar, and FRP rebar ratio, were selected as input parameters. At the same time, the punching shear capacity was the output parameter. The most important point in the modeling process of artificial neural networks is to choose a network with fewer neurons and higher regression. Thus, by evaluating the values of mean square error and regression for different hidden neurons, the network with 12 hidden neurons was chosen as the optimum one. The ANN and GMDH models with absolute fractions of variance (R^2) of 0.88 and 0.997 and mean absolute percentage error (MAPE)s of 8.05 and 4.32, respectively, showed acceptable predictions with high accuracy. However, the GMDH model was more precise in predicting the results, due to its lower MAPE values with its R^2 values being closer to one.

Furthermore, the sensitivity analyses were performed on both suggested models. In the ANN and GMDH models, the parameters of the small dimension of the column and slab effective depth, with 18.64% and 53.58%, had the highest effects on the punching shear capacity of the RC slabs, respectively. In addition, the least contributing parameters on the slab punching shear were related to the concrete strength and the elastic modulus in GMDH and ANN, respectively. In fact, the results showed that the model is significantly affected by the geometrical properties of slabs rather than mechanical characteristics.

References

[1] Metwally IM. Prediction of punching shear capacities of two-way concrete slabs reinforced with FRP bars. HBRC J 2013;9:125–33. doi:10.1016/j.hbrcj.2013.05.009.

[2] Hassan M, Ahmed EA, Benmokrane B. Punching shear behavior of two-way slabs reinforced with FRP shear reinforcement. J Compos Constr 2015. doi:10.1061/(ASCE)CC.1943-5614.0000493.

[3] Durucan C, Anil Ö. Effect of opening size and location on the punching shear behavior of interior slab-column connections strengthened with CFRP strips. Eng Struct 2015. doi:10.1016/j.engstruct.2015.09.033.

[4] Azimi A. GMDH-Network to Estimate the Punching Capacity of FRP-RC Slabs. Soft Comput Civ Eng 2017;1:86–92. doi:10.22115/scce.2017.48352.

[5] Naderpour H, Rezazadeh Eidgahee D, Fakharian P, Rafiean AH, Kalantari SM. A new proposed approach for moment capacity estimation of ferrocement members using Group Method of Data Handling. Eng Sci Technol an Int J 2020;23:382–91. doi:10.1016/j.jestch.2019.05.013.

[6] Rezazadeh Eidgahee D, Rafiean AH, Haddad A. A Novel Formulation for the Compressive Strength of IBP-Based Geopolymer Stabilized Clayey Soils Using ANN and GMDH-NN Approaches. Iran J Sci Technol Trans Civ Eng 2020;44:219–29. doi:10.1007/s40996-019-00263-1.

[7] Rezazadeh Eidgahee D, Haddad A, Naderpour H. Evaluation of shear strength parameters of granulated waste rubber using artificial neural networks and group method of data handling. Sci Iran 2019;26:3233–44. doi:10.24200/sci.2018.5663.1408.

[8] Naderpour H, Fakharian P, Rafiean AH, Yourtchi E. Estimation of the Shear Strength Capacity of Masonry Walls Improved with Fiber Reinforced Mortars (FRM) Using ANN-GMDH Approach. J Concr Struct Mater 2016;1:47–59. doi:10.30478/JCSM.2016.48988.

[9] Hamed Akbarpour MA. Prediction of punching shear strength of two-way slabs using artificial neural network and adaptive neuro-fuzzy inference system. Neural Comput Appl 2016:1–12. doi:10.1007/s00521-016-2239-2.

[10] Hassan NZ, Osman MA, El-Hashimy AM,

Tantawy HK. Enhancement of punching shear strength of flat slabs using shear-band reinforcement. HBRC J 2018. doi:10.1016/j.hbrcj.2017.11.003.

[11] Akhundzada H, Donchev T, Petkova D. Strengthening of slab-column connection against punching shear failure with CFRP laminates. Compos Struct 2019. doi:10.1016/j.compstruct.2018.09.076.

[12] Marí A, Cladera A, Oller E, Bairán JM. A punching shear mechanical model for reinforced concrete flat slabs with and without shear reinforcement. Eng Struct 2018. doi:10.1016/j.engstruct.2018.03.079.

[13] Hamdy M, Saafan M, Elwan SK, Elzeiny SM, Abdelrahman A. Punching Shear Behavior of RC Flat Slabs Strengthened with Steel Shear Bolts. Int J Curr Eng Technol 2018. doi:10.14741/ijcet/v.8.3.20.

[14] Gokkus U, Yildirim M, Yilmazoglu A. Prediction of Concrete and Steel Materials Contained by Cantilever Retaining Wall by Modeling the Artificial Neural Networks. J Soft Comput Civ Eng 2018;2:47–61. doi:10.22115/scce.2018.137218.1078.

[15] Wu X, Yu S, Xue S, Kang THK, Hwang HJ. Punching shear strength of UHPFRC-RC composite flat plates. Eng Struct 2019. doi:10.1016/j.engstruct.2019.01.099.

[16] Naderpour H, Nagai K, Fakharian P, Haji M. Innovative models for prediction of compressive strength of FRP-confined circular reinforced concrete columns using soft computing methods. Compos Struct 2019;215:69–84. doi:10.1016/j.compstruct.2019.02.048.

[17] Azizi R, Talaeitaba SB. Punching shear strengthening of flat slabs with CFRP on grooves (EBROG) and external rebars sticking in grooves. Int J Adv Struct Eng 2019. doi:10.1007/s40091-019-0218-4.

[18] Darvishan E. Prediction of the Lateral Confinement Coefficient of The concrete Columns Confined by FRP using the Artificial Neural Network. Concr Res 2020;13:67–80. doi:10.22124/jcr.2020.12174.1335.

[19] Fakharian P, Naderpour H, Haddad A, Rafiean AH, Rezazadeh ED. A Proposed Model for Compressive Strength Prediction of FRP-Confined Rectangular Columns in terms of Genetic Expression Programming (GEP). Concr Res 2018. doi:10.22124/jcr.2018.7162.1191.

[20] Li X, Khademi F, Liu Y, Akbari M, Wang C, Bond PL, et al. Evaluation of data-driven models for predicting the service life of concrete sewer pipes subjected to corrosion. J Environ Manage 2019;234:431–9. doi:10.1016/j.jenvman.2018.12.098.

[21] Hasanzade-Inallu A, Zarfam P, Nikoo M. Modified imperialist competitive algorithm-based neural network to determine shear strength of concrete beams reinforced with FRP. J Cent South Univ 2019;26:3156–74. doi:10.1007/s11771-019-4243-z.

[22] Naderpour H, Fakharian P, Hosseini F. Prediction of Behavior of FRP-Confined Circular Reinforced Concrete Columns using Artificial Neural Network. 8th Natl Conf Concr, Tehran, Iran: 2016. doi:10.13140/RG.2.2.11714.58568.

[23] ACI 318-11. Building code requirements for structural concrete (ACI318-11). 2011.

[24] British Standard. Structural use of concrete - Part 1. Code of practice for design and construction 1997:1–128.

[25] Committee ACI 440. Guide for the Design and Construction of Concrete Reinforced with FRP Bars (ACI 440.1 R-06). Am Concr Institute, Detroit, Michigan 2006.

[26] El-Ghandour AW, Pilakoutas K, Waldron P. Punching Shear Behavior of Fiber Reinforced Polymers Reinforced Concrete Flat Slabs: Experimental Study. J Compos Constr 2003;7:258–65. doi:10.1061/(ASCE)1090-0268(2003)7:3(258).

[27] Matthys S, Taerwe L. Concrete slabs reinforced with FRP grids. II: Punching resistance. J Compos Constr 2000;4:154–61.

[28] Ospina CE, Alexander SDB, Roger Cheng

JJ. Erratum: Punching of Two-Way Concrete Slabs with Fiber-Reinforced Polymer Reinforcing Bars or Grids (ACI Structural Journal (September-October 2003) 100:5). ACI Struct J 2003;100:834.

[29] El-Gamal S, El-Salakawy E, Benmokrane B. Behavior of concrete bridge deck slabs reinforced with fiber-reinforced polymer bars under concentrated loads. ACI Struct J 2005;102:727–35.

[30] Banthia N, Al-Asaly M, Ma S. Behavior of concrete slabs reinforced with fiber-reinforced plastic grid. J Mater Civ Eng 1995;7:252–7.

[31] Lee JH, Yoon YS, Cook WD, Mitchell D. Improving punching shear behavior of glass fiber-reinforced polymer reinforced slabs. ACI Struct J 2009;106:427–34.

[32] Ahmad SH, Zia P, Yu TJ, Xie Y. Punching Shear Tests of Slabs Reinforced with 3-Dimensional Carbon Fiber Fabric. Concr Int 1994;16:36–41.

[33] El-Salakawy E, Benmokrane B. Serviceability of concrete bridge deck slabs reinforced with fiber-reinforced polymer composite bars. ACI Struct J 2004;101:727–36. doi:10.14359/13395.

[34] Rahman AH, Kingsley CY, Kobayashi K. Service and ultimate load behavior of bridge deck reinforced with carbon FRP grid. J Compos Constr 2000;4:16–23.

[35] Hassan T, Abdelrahman a, Tadros G, Rizkalla S. Fibre reinforced polymer reinforcing bars for bridge decks. Can J Civ Eng 2000;27:839–49. doi:10.1139/l99-098.

[36] Hussein A, Rashid I, Benmokrane B. Two-way concrete slabs reinforced with GFRP bars. Adv Compos Mater Bridg Struct Proceeding 4th Int Conf Adv Compos Mater Bridg Struct CSCE, Calgary, Alta, Canada, July, 2004, p. 20–3.

[37] Ayish M. Punching shear behavior of flat plates with fiber reinforced concrete. Proc Int Conf on, Compos Constr 2004.

[38] Bouguerra K, Ahmed EA, El-Gamal S, Benmokrane B. Testing of full-scale concrete bridge deck slabs reinforced with fiber-reinforced polymer (FRP) bars. Constr Build Mater 2011;25:3956–65. doi:10.1016/j.conbuildmat.2011.04.028.

[39] Ramzy Z, Mahmoud Z, Salma T. Punching behavior and strength of two-way concrete slab reinforced with glass-fiber reinforced polymer (GFRP) rebars. Struct Compos Infrastructures Appl Conf 2007.

[40] Dulude C. Poinçonnement des dalles bidirectionnelles en béton armé d'armature de polymères renforcés de fibres de verre. Université de Sherbrooke; 2011.

[41] Hassan M, Ahmed E, Benmokrane B. Punching-Shear Strength of Normal and High-Strength Two-Way Concrete Slabs Reinforced with GFRP Bars. J Compos Constr 2013;17:04013003. doi:10.1061/(ASCE)CC.1943-5614.0000424.

[42] Nguyen-Minh L, Rovňák M. Punching shear resistance of interior GFRP reinforced slab-column connections. J Compos Constr 2012;17:2–13.

[43] Flood I. Next generation artificial neural networks and their application to civil engineering. Work Eur Gr Intell Comput Eng, 2006, p. 206–21.

[44] Kurnaz TF, Kaya Y. A novel ensemble model based on GMDH-type neural network for the prediction of CPT-based soil liquefaction. Environ Earth Sci 2019. doi:10.1007/s12665-019-8344-7.

[45] Milne L. Feature selection using neural networks with contribution measures. Aust Conf Artif Intell AI'95, Citeseer; 1995, p. 1–8.